



OPEN

Modeling and simulation of high energy density lithium-ion battery for multiple fault detection

Chandrani Sadhukhan¹, Swarup Kumar Mitra², Suvanjan Bhattacharyya^{3✉},
Eydah Almatrafi^{4,5,6}, Bahaa Saleh⁷ & Mrinal Kanti Naskar⁸

Lithium-ion battery, a high energy density storage device has extensive applications in electrical and electronic gadgets, computers, hybrid electric vehicles, and electric vehicles. This paper presents multiple fault detection of lithium-ion battery using two non-linear Kalman filters. A discrete non-linear mathematical model of lithium ion battery has been developed and Unscented Kalman filter (UKF) is employed to estimate the model parameter. Occurrences of multiple faults such as over-charge, over-discharge and short circuit faults between inter cell power batteries, affects the parameter variation of system model. Parallel combinations of some UKF (bank of filters) compare the model parameter variation between the normal and faulty situation and generates residual signal indicating different fault. Simulation results of multiple numbers of statistical tests have been performed for residual based fault diagnosis and threshold calculation. The performance of UKF is then compared with Extended Kalman filter (EKF) with same battery model and fault scenario. The simulation result proves that UKF model responses better and quicker than that of EKF for fault diagnosis.

The battery, an energy source has been used by the mankind since its invention more than two hundred years ago. After lots of developments, now-a-days batteries available are lighter in weight, higher energy storage capacity, enhanced safety features, and longer durability and found suitability in wide range of consumer and industrial applications^{1,2}. Lithium batteries have been modified into lithium ion to make it rechargeable and applied in electrical gadgets, computers, hybrid electric vehicles, and electric vehicles etc. Considering the aspects like reliability and safety of electric vehicles, it is important to monitor the states of lithium ion cells during operation. This can be managed by collection of required data and subsequent estimation of states of cells through a battery management system (BMS)^{3,4}. The performance of battery cell depends on current, voltage and temperature, and the state of cells include state of charge (SOC)⁵⁻⁷, state of health (SOH)⁸⁻¹⁰ and state of energy (SOE)¹¹ and remaining useful life time (RUL)^{12,13}. The faults in electrical vehicle are indicated as (a) overcharge, (b) over-discharge (c) internal and external short circuit. The battery internal and external short circuit fault results in generation of huge amount of heat which induces thermal runaway. Unchecked faults in the battery are irreversible in nature and may lead to damages when it is severe^{14,15}. In order to nullify such situations, it is important to diagnose fault of the battery quickly and accurately. It has been observed from the literatures that diagnosis of fault of lithium ion battery is of growing interest among researchers both in industry and academic field. The efforts have been put by the researchers aiming to detect different battery faults using advanced methodologies and techniques. One such technique is observer-based fault diagnosis which offers improved robustness because of its capability to avoid battery fault information loss. That may be accomplished due to unknown disturbances and faulty initial condition. The inherent advantages of lower cost and high flexibility make the model based fault diagnosis techniques a viable solution for accurate fault diagnosis¹⁶. The Luenberger observer (LO) using a

¹Electrical Engineering Department, MCKV Institute of Engineering, Liluah, Howrah, West Bengal 712104, India. ²Electronic & Telecommunication Engineering Department, MCKV Institute of Engineering, Liluah, Howrah, West Bengal 712104, India. ³Department of Mechanical Engineering, Birla Institute of Technology & Science, Pilani, Pilani Campus, VidyaVihar, Rajasthan 333 031, India. ⁴Mechanical Engineering Department, College of Engineering Rabigh, King Abdulaziz University, Jeddah, Saudi Arabia. ⁵K. A. CARE Energy Research and Innovation Centre, King Abdulaziz University, Jeddah 21589, Saudi Arabia. ⁶Center of Excellence in Renewable Energy and Power System, King Abdulaziz University, Jeddah, Saudi Arabia. ⁷Mechanical Engineering Department, College of Engineering, Taif University, P.O. Box 11099, Taif 21944, Saudi Arabia. ⁸Electronic & Telecommunication Engineering Department, Jadavpur University, Jadavpur, West Bengal 700032, India. ✉email: suvanjan.bhattacharyya@pilani.bits-pilani.ac.in

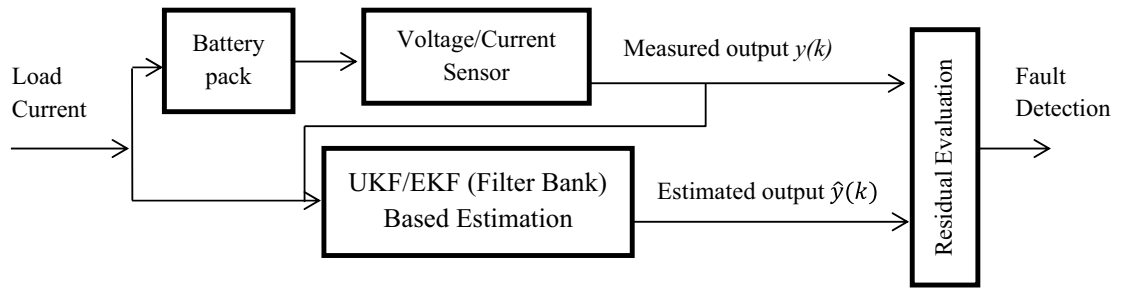


Figure 1. Schematic diagram of UKF/EKF bank-based fault detection scheme.

series of reduced order observers¹⁷ can be applied on battery-pack for fault detection. Some researchers proposed model-based short circuit fault analysis using advanced techniques like indentation¹⁸, nail penetration¹⁹, fabrication with defect structures²⁰ and thermal runaway at extreme high temperatures²¹. In another model, output voltages and the actual output voltages of batteries can be compared during the EV operation process and the alarm system will be triggered when the absolute value of the voltage difference exceeds the threshold^{22,23}. Also, Kalman filter finds its effective application for diagnosis of the fault in lithium-ion batteries^{24,25} in particular when optimal filter exhibits strong robustness with noisy signal. The model based fault detection methods facilitated with very high robustness can be used to detect faults of battery accurately. Adaptive Kalman filter based fault diagnosis for lithium ion battery is under consideration by many researchers^{26–28}. Adaptive Kalman filter can estimate states of battery parameter by the process and measurement noise covariance adjusting which is not possible in case of Extended Kalman filter where information on noise statistics are considered to be the prerequisite for proper functioning of the filter otherwise it may lead to inaccurate results. Recently overcharge and overdischarge of battery fault is discussed²⁹. A review paper on Fault Mechanisms, Fault Features, and Diagnosis Procedures are discussed³⁰.

Considering the wide application of lithium-ion batteries in various devices, it is desirable to manufacture batteries which will have higher energy density, power density and service life. The failure due to over-charge, over-discharge, short circuit between inter cells of lithium-ion battery could lead to performance degradation and system fault which in turn may cause inconvenience, faster aging and higher cost of maintenance, thermal runaway or even explosion. Therefore, it is imperative to design a reliable and robust battery management system for early detection of the faults of the battery during service condition. The overall performance is greatly dependent on critical functions such as State-of-Charge (SOC) and State-of-Health (SOH) estimations, over-charge, and under-charge protections etc. From the practical point of view, estimation of three faults, namely over-charge, over-discharge and short circuit fault between inter cell power of lithium-ion batteries will certainly improve the reliability and efficiency of the devices, gadgets, electric and hybrid electric vehicles etc.

It has been found that some published research papers concentrate only internal short circuit fault^{18–20} of the battery pack and some other works describes fault such as over-charge, over-discharge etc. No researcher has considered all these faults simultaneously of lithium-ion battery in their work using model based method. Most of the researchers have concentrated model based method using a single technique that is residual evaluation for estimation of the faults of the batteries^{22,24–26}. The novelty of present work is to model based fault detection occurs on lithium-ion battery pack for over-charge, over discharge and short circuit fault between inter cell power of lithium-ion batteries simultaneously. In the present study, a systematic model based fault detection scheme is proposed using a bank of Unscented Kalman filter (UKF) on lithium ion battery pack model for multiple fault detection such as over-charge, over-discharge and short circuit fault between inter cell power of lithium-ion batteries. A statistical test has been performed for residual based fault diagnosis and threshold calculation. The performance of UKF then compared with bank of Extended Kalman filter (EKF) on same battery model with same fault scenario. Depending on battery usage, different model of battery such as experimental, empirical, electrochemical are used. The battery model is considered as an extension of the The venin model where over-charged, over-discharged and short circuit fault between inter cell power of lithium-ion batteries are taken as fault parameter. The proposed work is divided into two parts: (a) experimental (b) simulation. In experimental part battery cells are monitored offline for long time interval in case of over-charging and over-discharging and parameter variation due to over-charging, over-discharging are measured. A 123 26650 LiFePO₄ battery (3.3 Volts, 2.5 Ah) cell was used in the experiment. Electrochemical impedance spectroscopy (EIS) technique is used to extract the circuit parameter variation during overcharging and discharging of the battery which is reflected in Tables 2 and 3. The parameter variations are incorporated in the battery model during simulation and run by two bank of filter such as UKF and EKF. The lithium ion battery states are estimated and also residual signal is generated by comparing estimated and measured output for each individual power cell using UKF bank. It has been shown that the UKF based fault diagnosis proves significant result when compared with EKF based approach.

Proposed fault diagnosis scheme on battery pack using UKF/EKF bank

A model-based fault detection scheme for a battery pack using bank of UKF or EKF is represented in Fig. 1. To diagnose the fault due to overcharge, over discharge or short circuit fault in a battery pack, a bank of UKF or EKF works in parallel with the system. A series of voltage and current sensors are connected to the battery pack to measure voltage and current in each cell of battery pack. The various parameters, states of battery model can

be measured by sensor provided data. The state space model of equivalent battery pack is designed and UKF or EKF banks are processed to get the estimated states of the system. The estimated data from filter and sensor provided data are compared and residual signal is generated. The mean of residual signal indicate the existence of fault in the system.

Residual signal generation. The discrete state space model of any non-linear time invariant system (with fault) can be expressed as

$$x(k + 1) = f(x(k), u(k)) + F_T(k), \tag{1}$$

$$y(k) = g(x(k), u(k)), \tag{2}$$

where, $x(k)$, $u(k)$ and $y(k)$ denotes the state vector, input signal and system output vector respectively at time step k . Nonlinear functions $f()$ and $g()$ are continuously differentiable with respect to time and $F_T(k)$ implies the occurrences of fault at time step k .

The discrete state space model of nonlinear Kalman Filter is given by

$$\hat{x}(k + 1) = f(\hat{x}(k), u(k)) + w(k), \tag{3}$$

$$\hat{y}(k) = g(\hat{x}(k), u(k)) + v(k), \tag{4}$$

where, $\hat{x}(k)$ and $\hat{y}(k)$ denotes estimated state vector and estimated output vector of the filter at time step k respectively. Where $w(k)$ and $v(k)$ are independent zero mean Gaussian process and measurement noise. The process noise variance Q_k and measurement noise variance R_k are expressed as.

$$E[w_i w_j^T] = \begin{cases} Q_k & i = j \\ 0 & i \neq j \end{cases}, \tag{5}$$

$$E[v_i v_j^T] = \begin{cases} R_k & i = j \\ 0 & i \neq j \end{cases}. \tag{6}$$

From Eq. (2) and Eq. (4), the residual signal is expressed as

$$\begin{aligned} r_d &= y(k) - \hat{y}(k) \\ &= F(w(k), v(k)) + F_T(k), \end{aligned} \tag{7}$$

where $F()$ is function of process $w(k)$ and measurement noise $v(k)$ sequence.

$$r_d = \begin{cases} F(w(k), v(k)) & (\text{healthy as } F_T(k) = 0) \\ F(w(k), v(k)) + F_T(k) & (\text{faulty as } F_T(k) \neq 0) \end{cases}. \tag{8}$$

If there exist any fault in the system $F_T(k)$, the filter output indicates the non-zero mean (NZM) residual sequences which is the summation of Gaussian noise and existing fault as given in Eq. (7). Simultaneous occurrences of multiple faults in the system each state of the filter output is indicated by NZM residual sequences.

A multiple fault diagnosis scheme is explained in the flowchart as shown in Fig. 2. When a system is affected by n number of different faults such as $F_{T1}, F_{T2}, \dots, F_{Tn}$, a bank of filters are utilized by incorporating each fault separately. The discrete state equation of each filter is represented as:

$$\left. \begin{aligned} \hat{x}_1(k + 1) &= f(\hat{x}_1(k), u(k)) + F_{T1} \\ \hat{x}_2(k + 1) &= f(\hat{x}_2(k), u(k)) + F_{T2} \\ &\vdots \\ \hat{x}_n(k + 1) &= f(\hat{x}_n(k), u(k)) + F_{Tn} \end{aligned} \right\}. \tag{9}$$

The output equation of each filter are described by

$$\left. \begin{aligned} \hat{y}_1(k) &= g(\hat{x}_1(k), u(k)) \\ \hat{y}_2(k) &= g(\hat{x}_2(k), u(k)) \\ &\vdots \\ \hat{y}_n(k) &= g(\hat{x}_n(k), u(k)) \end{aligned} \right\}. \tag{10}$$

The residual of each filter is the difference between the system output and the filtered output. Residual of each filter are expressed as

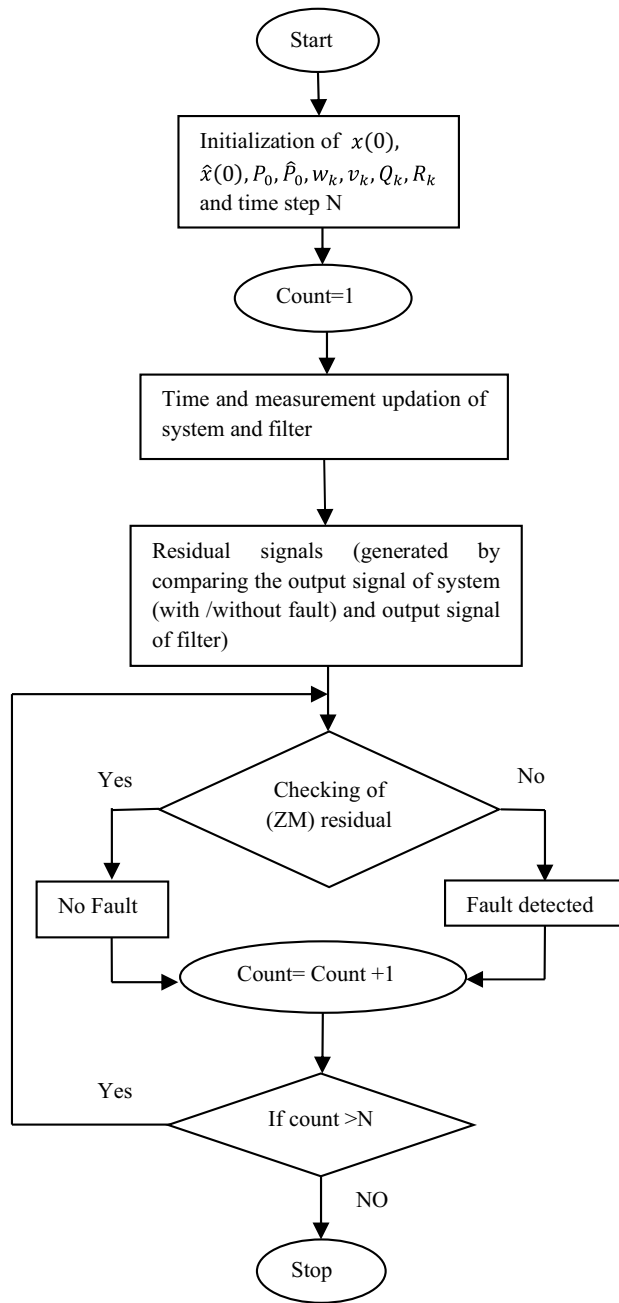


Figure 2. Residual based multiple fault diagnosis algorithm using UKF/EKF.

$$\left. \begin{aligned} r_{d1} &= y_1(k) - \hat{y}_1(k) \\ r_{d2} &= y_2(k) - \hat{y}_2(k) \\ &\vdots \\ r_{dn} &= y_n(k) - \hat{y}_n(k) \end{aligned} \right\} \quad (11)$$

The summary of UKF algorithm is given in Table 1. Residual based multiple fault diagnosis using UKF/EKF is shown in the flowchart given in Fig. 2. For *i* no. of cells are monitored by voltage or current sensor, if any fault occurs, the estimated state of filter output will not match with the sensor output data as a result Non Zero Mean (NZM) residual signal obtained. When fault does not occur in the system it shows output as Zero Mean (ZM) residual of process and measurement noise.

Filter Initialization:

$$x^+(0) = E[x(0)]P_0^+ = E[(x(0) - \hat{x}^+(0))(x(0) - \hat{x}^+(0))^T]$$

Sigma vector generation:

$$\left. \begin{aligned} X_{k-1}^0 &= \hat{x}^+(k-1) \\ X_{k-1}^i &= \hat{x}^+(k-1) + (\sqrt{(n+\lambda)}c_i) \\ X_{k-1}^{i+n} &= \hat{x}^+(k-1) - (\sqrt{(n+\lambda)}c_i) \end{aligned} \right\} 1 \leq i \leq n$$

Weighting vector generation

$$\begin{aligned} W_0^m &= \frac{\lambda}{n+\lambda} \\ W_0^c &= \frac{\lambda}{n+\lambda} + (1 - \sigma^2 + \beta) \\ W_i^m = W_i^c &= \frac{1}{2(n+\lambda)} \quad i = 1, 2, \dots, 2n \end{aligned}$$

Time updation

$$\hat{x}^-(k) = \sum_{i=0}^{2n} W_i^m X_{k-1}^i, \quad P_k^- = \sum_{i=0}^{2n} W_i^c (X_{k-1}^i - \hat{x}^-(k))(X_{k-1}^i - \hat{x}^-(k))^T + Q,$$

Measurement updation

$$\hat{y}(k) = \sum_{i=0}^{2n} W_i^m \hat{y}_k^i, \quad P_y \approx \sum_{i=0}^{2n} W_i^c (\hat{y}_k^i - \hat{y}(k))(\hat{y}_k^i - \hat{y}(k))^T + R_k,$$

Kalman gain

$$\begin{aligned} K_k &= P_{xy}P_y^{-1}, \quad P_{xy} = \sum_{i=0}^{2n} W_i^c (\hat{X}_k^i - \hat{x}(k))(\hat{y}_k^i - \hat{y}(k))^T \\ \hat{x}(k) &= \hat{x}^-(k) + K_k(y(k) - \hat{y}(k)), \quad P_k^+ = P_k^- - K_kP_yK_k^T \end{aligned}$$

Table 1. Summary of UKF algorithm.

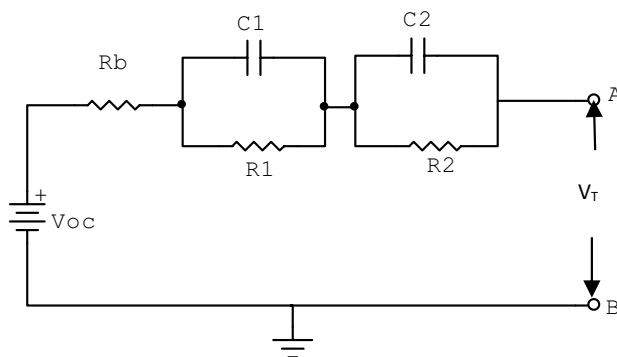


Figure 3. Equivalent circuit model of the battery pack.

Battery modeling

Model based fault diagnosis method is implemented using electrochemical properties of a battery. An extension of the venin model is presented which is already applied for various fault diagnosis and state estimation problem. The extended model is used because of the complexity in computation of partial differential equations in electrochemical models. A second order battery model of an additional RC parallel circuit element as shown in Fig. 3 is considered to represent the electrochemical phenomenon of cells. The parameters are interfacial impedance, reactivity distribution of the electrode and the resistance of electron and ion migration. The equivalent circuit

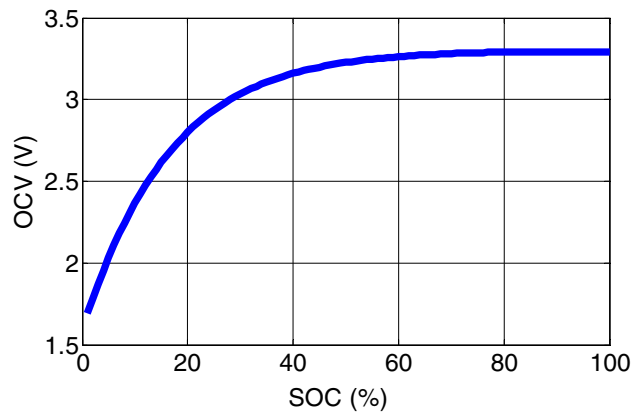


Figure 4. OCV-SOC characteristic for LiFePO₄ battery cell.

consists of a controlled or open circuit voltage source V_{oc} and change in its value with the SOC, a resistor R_b denotes the bulk electrolyte resistance which can vary during the process of charging/ discharging. The constant phase element (C_1) and resistance (R_1) makes resistor–capacitor (RC) networks used as model of reactivity capturing model of electrode and the other second RC network combination of R_2 and C_2 denote the resistance and capacitance of charge transfer respectively. The current (I) shows charging/discharging current of the system, the performance of a battery pack is greatly affected by the parameters like current, internal resistance and terminal voltage. These parameters are responsible to regulate inconsistency quality, the mode of connection, the variable capacity of cells at different discharge current rate, etc. The resistance–capacitance electrical circuits can be used to model a third order system for battery cells. The each elements of the circuit are the function of SOC and temperature. In the present study the temperature is kept constant, the voltage is varied as a function of SOC and aging dynamics have been kept aside in the model. The significant aspect to be considered is that, the signature fault which may occur in the battery while in operation can be modeled to study behavior of the system under abnormal situations. Effective control of fault estimation also improves the battery life to a large extent. The failure of battery due to overcharging leads to generation of excessive heat due to increase in temperature may cause violent thermal runaways. Moreover, the detrimental copper plating which occurs at the negative electrode of the battery significantly influences the failure of over discharging leading to further thermal runaways. Different types of variation in parameters are noticed during failure of the battery cells due to overcharging and over discharging. It is observed that the increase in bulk resistance (R_b) is more during overcharging than that of over discharging. Also, the charge transfer resistance (R_1 , R_2) varies proportionally with both overcharging and over discharging condition. The variation of double layer capacitance (C_1) and the charge transfer capacitor (C_2) show a steep increase with over discharging, but the same is very small with gradual dipping in nature is seen in case of overcharging.

The dynamic equations of the equivalent model of the battery can be represented by

$$\dot{V}_1(t) = -\frac{1}{R_1 C_1} V_1(t) + \frac{1}{C_1}, \quad (12)$$

$$\dot{V}_2(t) = -\frac{1}{R_2 C_2} V_2(t) + \frac{1}{C_2}, \quad (13)$$

$$V_T(t) = V_{OC}(t) - V_1(t) - V_2(t) - I(t)R_b, \quad (14)$$

where, V_T , V_1 and V_2 denote the terminal voltage and capacitor voltage across C_1 and C_2 respectively. Open circuit voltage V_{oc} is a nonlinear function of SOC and described by

$$V_{OC}(t) = \sum_{k=0}^m C_k SOC^k(t), \quad (15)$$

where, coefficients C_k , for $k=0,1,2,\dots,m$ are obtained from OCV-SOC characteristic shown in Fig. 4.

The SOC, calculated by the coulomb counting method is given as:

$$\frac{dSOC(t)}{dt} = \frac{\eta I_b}{C_a},$$

$$\text{or } SOC(t) = SOC(0) + \int_0^t \frac{\eta I_b(\tau)}{C_a} d\tau, \quad (16)$$

Cycle	R_b (Ω)	C_1 (F)	R_2 (Ω)	C_2 (F)	R_1 (Ω)
1	0.0771	0.0265	0.0156	0.4177	0.0282
5	0.2433	0.00041	0.0369	0.2463	0.0329
10	0.1387	0.00012	0.1429	0.3421	0.0342
12	0.1661	0.0001	0.1734	0.3657	0.0389
15	0.2865	0.0007	0.2134	0.3867	0.04327

Table 2. Variation of system parameters (over-charge).

Cycle	R_b (Ω)	C_1 (F)	R_2 (Ω)	C_2 (F)	R_1 (Ω)
1	0.0771	0.0265	0.0156	0.4177	0.0282
5	0.2433	0.00041	0.0369	0.2463	0.0329
10	0.1387	0.00012	0.1429	0.2567	0.0438
12	0.1661	0.00010	0.1654	0.3569	0.0541
15	0.2865	0.0007	0.1875	0.6541	0.0654

Table 3. Variation of system parameters (over-discharge).

where, C_a is the battery available capacity, and η is the coulomb efficiency that is the function of the current and temperature. $\eta = \begin{cases} 1 & \text{for charging} \\ 0.95 & \text{for discharging} \end{cases}$

The model parameter are kept constant neglecting changes occurred due to ageing effect. To simulate with the discrete Kalman filter, the filter model is discretized using Taylor series expansion and neglecting higher terms given as

$$V_1(k+1) = (e^{-t_s/R_1 C_1}) V_1(k) + R_1 (1 - e^{-t_s/R_1 C_1}) I_b(k), \quad (17)$$

$$V_2(k+1) = (e^{-t_s/R_2 C_2}) V_2(k) + R_2 (1 - e^{-t_s/R_2 C_2}) I_b(k), \quad (18)$$

$$SOC(k+1) = SOC(k) - \frac{\eta t_s I_b(k)}{C_a}, \quad (19)$$

$$\begin{aligned} V_T(k) &= V_{oc}(k) + V_1(k) + V_2(k) + R_b I_b(k) \\ &= C_7 SOC^7(k) + C_6 SOC^6(k) + C_5 SOC^5(k) + C_4 SOC^4(k) \\ &\quad + C_3 SOC^3(k) + C_2 SOC^2(k) + C_1 SOC(k) + C_0 + V_1(k) + V_2(k) + R_b I_b(k) \\ &= f(SOC(k)) + V_1(k) + V_2(k) + R_b I_b(k). \end{aligned} \quad (20)$$

These can be expressed as state variable form as

$$\begin{bmatrix} SOC(k+1) \\ V_1(k+1) \\ V_2(k+1) \end{bmatrix} = \begin{bmatrix} 1 & 0 & 0 \\ 0 & (e^{-t_s/R_1 C_1}) & 0 \\ 0 & 0 & (e^{-t_s/R_2 C_2}) \end{bmatrix} \begin{bmatrix} SOC(k) \\ V_1(k) \\ V_2(k) \end{bmatrix} + \begin{bmatrix} -\frac{\eta t_s}{C_a} \\ R_1 (1 - e^{-t_s/R_1 C_1}) \\ R_2 (1 - e^{-t_s/R_2 C_2}) \end{bmatrix} I_b(k), \quad (21)$$

$$V_T(k) = \begin{bmatrix} f(SOC(k)) & 1 & 1 \end{bmatrix} \begin{bmatrix} SOC(k) \\ V_1(k) \\ V_2(k) \end{bmatrix} + [R_b] I_b(k). \quad (22)$$

Simulation result and discussion

A 123 26650 LiFePO₄ battery (3.3 Volts, 2.5 Ah) cell was used in the experiment. Tables 2 and 3 illustrate the impedance spectroscopy results for the selected circuit parameters variation when the battery cell was under over-charge and over-discharge fault conditions. During over-charge condition battery cell is kept with 120% charge and 100% nominal discharge while during over-discharge condition it is kept in reverse way. In each fault condition spectroscopy measurement for parameter variation of some specific cycles are taken and shown in Tables 2 and 3. Various faults in lithium ion battery cells can be observed by different parameter variation in battery during operation. The paper primarily focused on over-charging (OC) fault, over-discharging (OD) fault and short circuit fault between inter cell power of lithium-ion batteries. The OC condition is achieved by charging the battery to 120% and 100% nominal discharge at a favorable current rate. The variation of system parameters

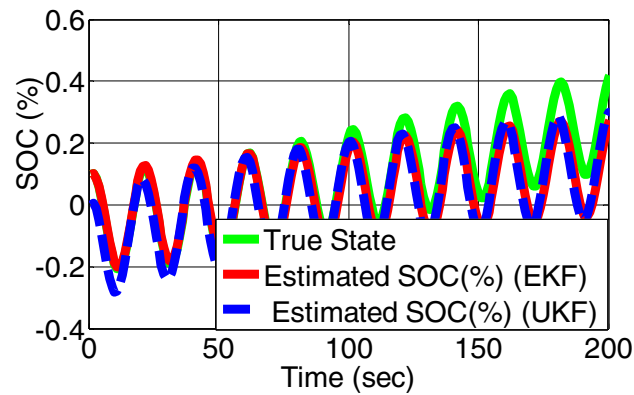


Figure 5. SOC estimation by EKF and UKF on simulated battery model.

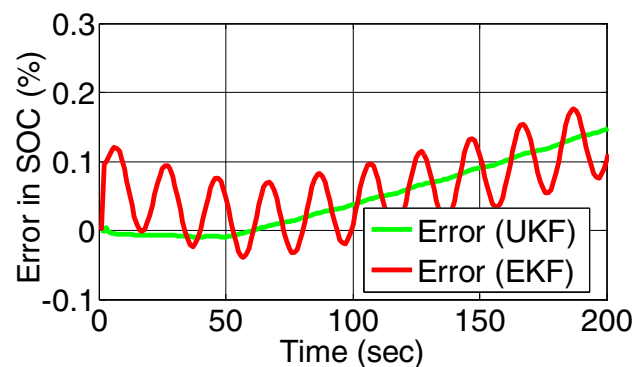


Figure 6. Error/residual evaluation for SOC estimation by EKF and UKF on simulated battery model.

such as R_b , R_1 , R_2 , C_1 and C_2 , which significantly contributed in faults during OC and over-discharging (OD) of battery cell parameter variation as seen in the impedance spectroscopy are shown in Tables 2 and 3.

Sinusoidal current as input signal is used as charging or discharging current of the model.

The terminal voltage, state of charge, voltage across C_1 and C_2 in each sampling time is evaluated from the Eqs. (21) and (22). The battery model is run by bank of UKF and EKF to calculate the estimated state of charge, voltage across C_1 and C_2 in each sampling time with healthy and faulty state while the input signal is corrupted with Gaussian white noise with process noise covariance Q_k and measurement noise covariance R_k are taken as

$$Q = 10^{-6} \begin{bmatrix} 1 & 0 & 0 \\ 0 & 1 & 0 \\ 0 & 0 & 1 \end{bmatrix} \text{ and } R = 1 \times 10^{-6} \text{ respectively.}$$

Simulation result deals with performance comparison between UKF and EKF while fault diagnosis of lithium ion battery of electric vehicle. Over-charging, over-discharging and short circuit faults are experimented in battery model and each case for fault diagnosis bank of UKF and EKF are operated. The three states of battery models, those are state of charge, voltage across C_1 and C_2 are estimated and compared to get residual signal in each time step.

The charging current is taken as input signal considered as $I = 5\sin 100\pi t$ with initial values of voltage across charge transfer capacitance and double layer capacitances are taken as 0.1 V each. The model is simulated with healthy condition and at 50th sampling instant a fault is injected as overcharge and at 120th sampling instant second fault occurs. As the system is modeled with three state variables as SOC, V_1 and V_2 , the occurrences of any fault will affect the states of battery model. By comparing the true state and estimated state during healthy and faulty condition is easily detected by residual signal generation.

Single fault diagnosis. In the proposed battery model is first run healthy condition and at 50th sampling instant a fault is injected as overcharge. Figure 5 represents the true state and estimated state of SOC by EKF and UKF. Figure 6 represents the residual of SOC of both the filter. For both cases the change of residual signal from zero to other value is more appropriate in UKF than EKF.

Figures 7 and 8 shows the estimated state of voltage across charge transfer capacitance and the residual signal of both the filter. The residual measurement and state estimation do not reflect the occurrences of fault as overcharge does not affect the voltage across charge transfer capacitances.

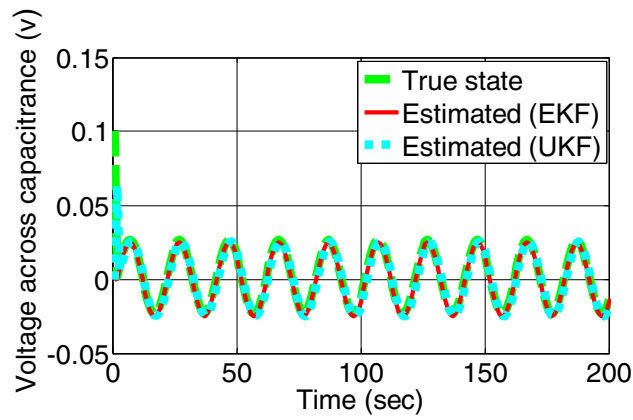


Figure 7. Voltage across charge transfer capacitance estimated by EKF and UKF during charging.

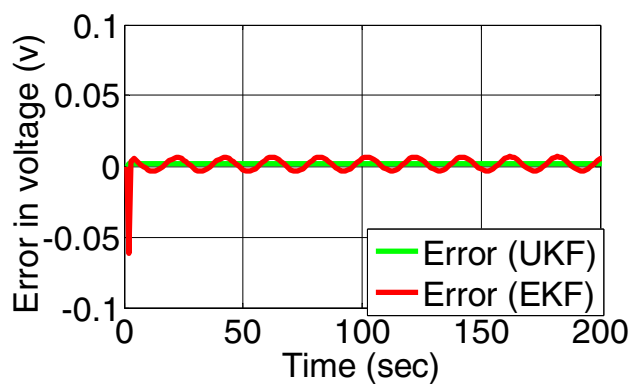


Figure 8. Error/residual evaluation for voltage across charge transfer capacitance estimation by EKF and UKF.

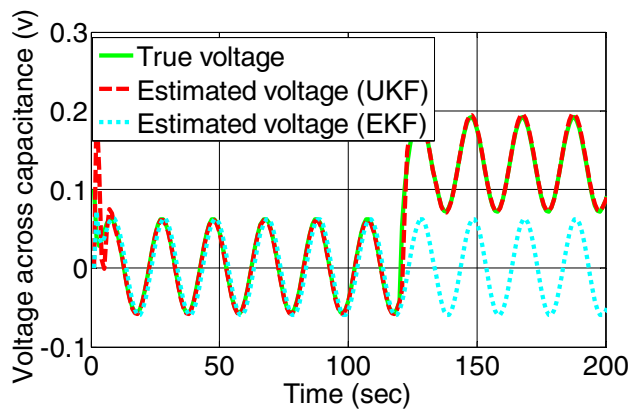


Figure 9. Voltage across charge transfer capacitance estimated by EKF and UKF during over discharging.

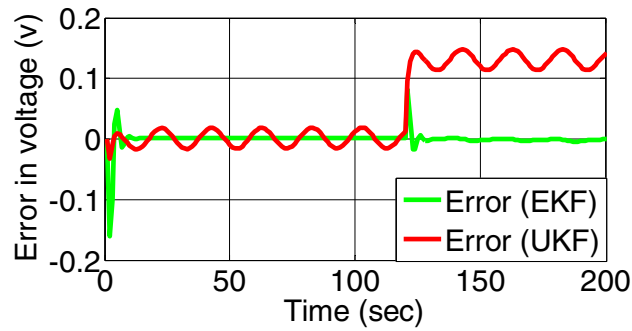


Figure 10. Error/residual evaluation for Voltage across charge transfer capacitance estimation by EKF and UKF during discharging.

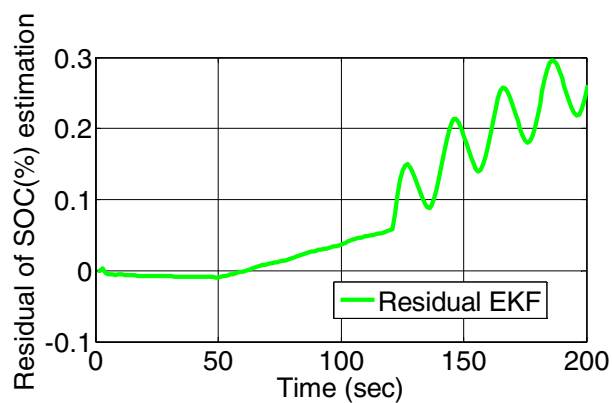
When over discharging fault occurs at 120th second, the true voltage and estimated voltage across charge transfer capacitance by both filters are represented by Fig. 9. The residual signal of both the filters is shown in Fig. 10.

The shift of residual for second fault is clear for UKF than EKF. Under this condition the residual for SOC is unaffected showing zero.

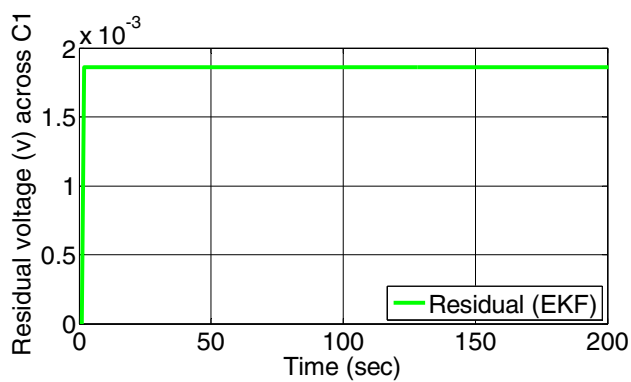
Multiple fault diagnosis. When overcharging fault at 50th s and short circuit fault across charge transfer resistance at 120th s both fault occurs on battery model simultaneously, the residual of SOC and voltage across charge transfer capacitance and double layer capacitance are depicted in Figs. 11a–c and 12a–c.

Conclusion

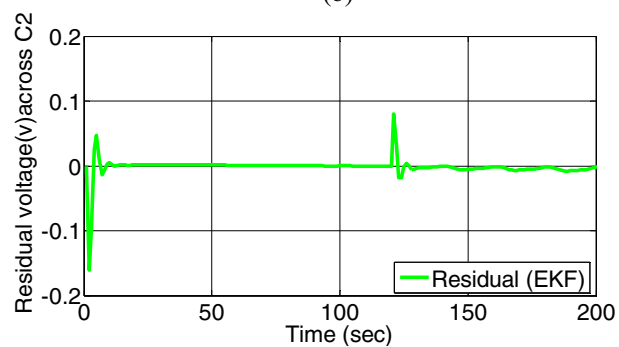
In the present study, a discrete non-linear mathematical model of lithium-ion battery has been developed for multiple fault detection using two non-linear Kalman filters. The performance comparison using bank of UKF and EKF for single and simultaneous occurrences of multiple fault diagnosis such as over-charge, over-discharge and short circuit fault between inter cell power in lithium-ion battery has been carried out. In the proposed fault diagnosis scheme both (UKF and EKF) bank of filters are employed separately on lithium-ion battery model during normal and faulty situation so that the filters output and measured output are compared to generate residual signals. It has been shown from the simulation results of statistical test that residual signal under no fault indicates zero mean signal within threshold value whereas it exceeds the threshold value with non-zero mean signal during faulty condition. The comparison result for both the filter (UKF and EKF) from simulation study proves that UKF model exhibits better and quicker response than that of EKF for multiple fault diagnosis of lithium-ion battery model.



(a)



(b)



(c)

Figure 11. (a) Residual estimation of SOC, (b) residual estimation of voltage across charge transfer capacitance. (c) Residual estimation of voltage across double layer capacitance by EKF.

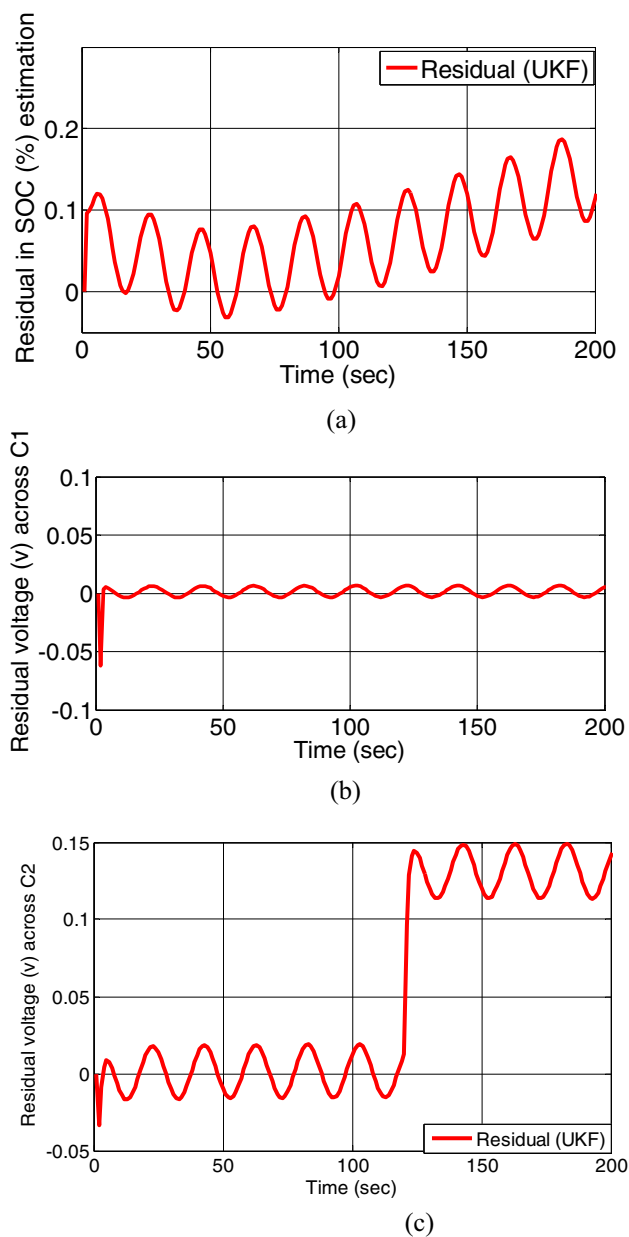


Figure 12. (a) Residual estimation of SOC, (b) residual estimation of voltage across charge transfer capacitance, (c) residual estimation of voltage across double layer capacitance by UKF.

Data availability

All data generated or analysed during this study are included in this published article.

Received: 12 January 2022; Accepted: 5 April 2022

Published online: 13 June 2022

References

1. Tarascon, J. M. & Armand, M. Issues and challenges facing rechargeable lithium batteries. *Nature* **414**, 359–367 (2001).
2. Goonan, T. G. *Lithium use in batteries*. U. S. G. Survey (2012). <http://pubs.usgs.gov/circ/1371/>.
3. Lu, L., Han, X., Li, J., Hua, J. & Ouyang, M. A review on the key issues for lithium-ion battery management in electric vehicles. *J. Power Sources* **226**, 272–288. <https://doi.org/10.1016/j.jpowsour.2012.10.060> (2013).
4. Bergveld, H. J., Kruijt, W. S. & Notten, P. H. L. *Battery Management Systems Design by Modelling* (Springer, 2002).
5. Wei, Z., Zou, C., Leng, F., Soong, B. H. & Tseng, K. J. Online model identification and state of charge estimate for lithium-ion battery with a recursive total least squares based observer. *IEEE Trans. Ind. Electron.* **65**, 1336–1346 (2017).
6. Cheng, K. W. E., Divakar, B. P., Wu, H., Ding, K. & Ho, H. F. Battery-management system (BMS) and SOC development for electrical vehicles. *IEEE Trans. Veh. Technol.* **60**(1), 76–88 (2011).

7. Wang, Y., Zhang, C. & Chen, Z. A method for joint estimation of state-of-charge and available energy of LiFePO₄ batteries. *Appl. Energy* **135**, 81–87 (2014).
8. Bartlett, A., Marcicki, J., Rhodes, K. & Rizzoni, G. State of health estimation in composite electrode lithium-ion cells. *J. Power Sources* **284**, 642–649 (2015).
9. Andre, D., Appel, C., Soczka-Guth, T. & Sauer, D. U. Advanced mathematical methods of SOC and SOH estimation for lithium-ion batteries. *J. Power Sources* **224**, 20–27 (2013).
10. Zou, C., Manzie, C., Nešić, D. & Kallapur, A. G. Multi-time-scale observer design for state-of-charge and state-of-health of a lithium-ion battery. *J. Power Sources* **335**, 121–130 (2016).
11. Wang, Y., Zhang, C. & Chen, Z. An adaptive remaining energy prediction approach for lithium-ion batteries in electric vehicles. *J. Power Sources* **305**, 80–88 (2016).
12. Dong, H., Jin, X., Lou, Y. & Wang, C. Lithium-ion battery state of health monitoring and remaining useful life prediction based on support vector regression-particle filter. *J. Power Sources* **271**, 114–123 (2014).
13. Wu, J., Zhang, C. & Chen, Z. An online method for lithium-ion battery remaining useful life estimation using importance sampling and neural networks. *Appl. Energy* **173**, 134–140 (2016).
14. Zhang, J. & Lee, J. A review on prognostics and health monitoring of Li-ion battery. *J. Power Sources* **196**, 6007–6014 (2011).
15. Goebel, K., Saha, B., Saxena, A., Celaya, J. & Christophersen, J. Prognostics in battery health management. *IEEE Instrum. Meas. Mag.* **11**, 33–40 (2008).
16. Ding, S. X. *Model-Based Fault Diagnosis Techniques: Design Schemes, Algorithms, and Tools* (Springer, 2008).
17. Chen, W., Chen, W. T., Saif, M., Li, M. F. & Wu, H. Simultaneous fault isolation and estimation of lithium-ion batteries via synthesized design of Luenberger and learning observers. *IEEE Trans. Control Syst. Technol.* **22**, 290–298 (2013).
18. Greve, L. & Fehrenbach, C. Mechanical testing and macro-mechanical finite element simulation of the deformation, fracture, and short circuit initiation of cylindrical Lithium ion battery cells. *J. Power Sources* **214**, 377–385 (2012).
19. Maleki, H. & Howard, J. N. Internal short circuit in Li-ion cells. *J. Power Sources* **191**, 568–574 (2009).
20. Orendor, C. J., Roth, E. P. & Nagasubramanian, G. Experimental triggers for internal short circuits in lithium-ion cells. *J. Power Sources* **196**, 6554–6558 (2011).
21. Feng, X. *et al.* Thermal runaway features of large format prismatic lithium ion battery using extended volume accelerating rate calorimetry. *J. Power Sources* **255**, 294–301 (2014).
22. Singh, A., Izadian, A. & Anwar, S. Model based condition monitoring in lithium-ion batteries. *J. Power Sources* **268**, 459–468 (2014).
23. Liu, Z. & He, H. Model-based sensor fault diagnosis of a lithium-ion battery in electric vehicles. *Energies* **8**, 6509–6527. <https://doi.org/10.3390/en8076509> (2015).
24. Singh, A., Izadian, A. & Anwar, S. Fault diagnosis of Li-ion batteries using multiple-model adaptive estimation. In *IEEE Ind. Electron. IECON 2013—39th Annual Conference of the IEEE Industrial Electronics Society, Vienna, Austria*. <https://doi.org/10.1109/IECON.2013.6699695> (2013).
25. Singh, A., Izadian, A. & Anwar, S. Nonlinear model based fault detection of lithium ion battery using multiple model adaptive estimation. In *19th IFAC World Congress, Cape Town, South Africa*. <https://doi.org/10.3182/20140824-6-ZA-1003.00711> (2014).
26. Sidhu, A., Izadian, A. & Anwar, S. Adaptive nonlinear model-based fault diagnosis of Li-ion batteries. *IEEE Trans. Ind. Electron.* **62**, 1002–1011 (2015).
27. Plett, G. L. Extended Kalman filtering for battery management systems of LiPB based HEV battery packs—Part 3. State and parameter estimation. *J. Power Sources* **134**, 277–292 (2004).
28. Hongwen, H., Xiong, R. & Guo, H. Online estimation of model parameters and state-of-charge of LiFePO₄ batteries in electric vehicles. *Appl. Energy* **89**, 413–420 (2012).
29. Zheng, T. Fault diagnosis of overcharge and overdischarge of lithium ion batteries. *Chem. Eng. Trans.* **71**, 1453–1458 (2018).
30. Hu, X. *et al.* Advanced fault diagnosis for lithium-ion battery systems: A review of fault mechanisms, fault features, and diagnosis procedures. *IEEE Ind. Electron. Mag.* **14**(3), 65–91 (2020).

Acknowledgements

The authors also acknowledge the support provided by King Abdullah City for Atomic and Renewable Energy (K.A. CARE) under K. A. CARE—King Abdulaziz University Collaboration Program.

Author contributions

Supervision: S.B.; M.K.N.; Writing—review & editing: S.B.; C.S.; Project administration: M.K.N.; S.K.M.; S.B.; Investigation: C. S.; S.B.; E.A.; B.S.; data curation: C.S.; S.K.M.; S.B.; B.S.; Writing: C.S.; S.K.M.; S.B.; E.A.; Methodology: C.S.; E.A.; Conceptualization: C.S.; S.B.; E.A.; M.K.N.; All authors have read and agreed to the published version of the manuscript.

Competing interests

The authors declare no competing interests.

Additional information

Correspondence and requests for materials should be addressed to S.B.

Reprints and permissions information is available at www.nature.com/reprints.

Publisher's note Springer Nature remains neutral with regard to jurisdictional claims in published maps and institutional affiliations.



Open Access This article is licensed under a Creative Commons Attribution 4.0 International License, which permits use, sharing, adaptation, distribution and reproduction in any medium or format, as long as you give appropriate credit to the original author(s) and the source, provide a link to the Creative Commons licence, and indicate if changes were made. The images or other third party material in this article are included in the article's Creative Commons licence, unless indicated otherwise in a credit line to the material. If material is not included in the article's Creative Commons licence and your intended use is not permitted by statutory regulation or exceeds the permitted use, you will need to obtain permission directly from the copyright holder. To view a copy of this licence, visit <http://creativecommons.org/licenses/by/4.0/>.

© The Author(s) 2022